Biochemistry

 Volume 39, Number 41 October 17, 2000

Articles

Akt-Dependent Antiapoptotic Action of Insulin Is Sensitive to Farnesyltransferase Inhibitor

Doekbae Park,‡ Sanjay K. Pandey, Elena Maksimova, Sutapa Kole, and Michel Bernier*

Diabetes Section, Laboratory of Clinical Investigation, National Institute on Aging, National Institutes of Health, 5600 Nathan Shock Drive, Box 23, Baltimore, Maryland 21224-6825

Received May 1, 2000; Revised Manuscript Received August 7, 2000

ABSTRACT: CHO cells expressing the human insulin receptors (IR) were used to evaluate the effect of the potent farnesyltransferase inhibitor, manumycin, on insulin antiapoptotic function. Cell treatment with manumycin blocked insulin's ability to suppress pro-apoptotic caspase-3 activity which led to time-dependent proteolytic cleavage of two nuclear target proteins. The Raf-1/MEK/ERK cascade and the serine/threonine protein kinase Akt are two survival pathways that may be activated in response to insulin. We tested the hypothesis that inhibition of farnesylated Ras was causally related to manumycin-induced apoptosis and showed that the response to manumycin was found to be independent of K-Ras function because membrane association and activation of endogenous K-Ras proteins in terms of GTP loading and ERK activation were unabated following treatment with manumycin. Moreover, blocking p21Ras/Raf-1/MEK/ERK cascade by the expression of a transdominant inhibitory mSOS1 mutant in CHO-IR cells kept cells sensitive to the antiapoptotic action of insulin. Insulin-dependent activation of Akt was blocked by 4 h treatment with manumycin ($P < 0.01$), a kinetic too rapid to be explained by Ras inhibition. This study suggests that the depletion of short-lived farnesylated proteins by manumycin suppresses the antiapoptotic action of insulin at least in part by disrupting Akt activation but not that of the K-Ras/Raf-1/ERK-dependent cascade.

Apoptosis is the most frequent morphological feature of programmed cell death thought to play a pivotal role in diverse physiological and pathological processes. These include homeostatic maintenance of tissues and organs, autoimmune diabetes and diabetic neuropathy (*1*, *2*). Insulin exerts protection against apoptotic death mediated by growth factor withdrawal in a number of cellular models (*3*−*7*). Despite recent advance in the identification of gene products involved in the prevention or induction of apoptosis (reviewed in ref *8*), the mechanisms by which insulin participates in this process remain largely unknown. Hence, investigating signaling pathways that are involved in insulin-mediated antiapoptotic protection shall play a crucial role in our understanding of insulin action.

Activation of the insulin receptor (IR) tyrosine kinase is essential for many of the biological actions of insulin. The liganded receptor initiates intracellular signals by stimulating tyrosine phosphorylation of endogenous substrates [e.g.,

* To whom correspondence should be addressed. Phone: (410) 558-8199. Fax: (410) 558-8381. E-mail: Bernierm@vax.grc.nia.nih.gov.
‡ Present address: Lab. Histology, College of Medicine, Cheju National University, Cheju, 690-756, Korea.

[1] Abbreviations: IR, insulin receptor; ERK, extracellular signal-regulated kinase; CHO, chinese hamster ovary; PI, propidium iodide; FACS, fluorescence-activated cell sorting; PAGE, polyacrylamide gel electrophoresis; SFM, serum-free medium; RBD, Ras binding domain; FTI, farnesyltransferase inhibitor; PARP, poly(ADP-ribose) polymerase.

10.1021/bi000995y CCC: $19.00
Published on Web 09/20/2000

insulin receptor substrate (IRS) and Shc proteins]. Tyrosine phosphorylation of IRS-1 allows compartmentalization of signaling molecules, including members of the class I phosphatidylinositol 3-kinase (PI 3-kinase) family (*9*). Insulin induces also the formation of a Shc-Grb2-SOS ternary complex that enables p21Ras activation (*10*, *11*). Expression of a mutant SOS protein that lacks the guanine nucleotide exchange domain causes a marked inhibition in the formation of GTP-bound p21Ras, thus atttenuating Ras-dependent insulin signaling pathway (*12*). p21Ras stimulates downstream effectors that participate in mitogen-activated protein (MAP) kinase activation, an essential route that conveys mitogenic signals to the nucleus. GTP-bound Ras triggers the recruitement of Raf-1 to the plasma membrane where its kinase activity is activated. This results in subsequent Raf-1-mediated phosphorylation and activation of the dual threonine/tyrosine kinase, MAP kinase kinase (MEK), which in turn phosphorylates and activates extracellular signal-regulated kinases (ERKs) (*13*). p21Ras and the 110 kDa catalytic subunit of class I PI 3-kinase are found within a protein complex in a GTP-dependent manner, indicating that Ras may also contribute to PI 3-kinase activation (*14*).

Farnesylation is a regulated posttranslational modification that allows attachement of a number of proteins, including p21Ras, to the plasma membrane. By inducing the activity of the enzyme farnesyl protein transferase, insulin increases the pool of membrane-associated p21Ras and promotes GTP loading on Ras (*15*, *16*). It has been recently documented that manumycin, a selective protein farnesylation inhibitor (FTI), blocks the antiapoptotic protection exerted by insulin in IR-expressing CHO cells maintained in the absence of growth factors (*17*). However, this study has not addressed the mechanism by which manumycin induces apoptotic death.

A limitation of FTIs as general anti-Ras agents is that Ras isoforms are differentially affected by inhibition of farnesyltransferase activity. Unlike H-Ras, K-Ras undergoes alternative lipid modification by geranylgeranyltransferases in cells treated with FTI (*18*, *19*), thus allowing this alternatively prenylated version of K-Ras to remain associated with the membrane fraction and be biologically active (*20*). Because Ras isoforms are known to exhibit differential activities toward the Raf-1/ERK cascade and the PI 3-kinase/Akt pathway (*21*), the pro-apoptotic action of manumycin may be the result of selective inhibition of either one of these survival signaling pathways. Using various experimental approaches, we report here that the K-Ras/Raf-1/ERK cascade was not the target of manumycin action, in contrast to the rapid decrease in insulin-stimulated Akt phosphorylation and activation in untransformed CHO-IR cells. Since engagement of H-Ras preferentially activates the PI 3-kinase/Akt pathway (*21*), we tested also the hypothesis that cellular expression of a dominant negative H-Ras mutant may mimic manumycin in its ability to promote apoptosis.

MATERIAL AND METHODS

Materials. Manumycin, FTI-277, porcine insulin, monoclonal antibodies against pan Ras and K-Ras, the fluorogenic caspase-3 substrate, Ac-DEVD-AMC, two caspase-3 inhibitors, z-DEVD-fmk and DEVD-CHO, and the caspase-3 colorimetric substrate, Ac-DEVD-*p*NA, were obtained from Calbiochem (La Jolla, CA). Bovine serum albumin (RIA grade), propidium iodide (PI), and anti-actin antibodies were from Sigma Chemical Corp. (St. Louis, MO). Protein G-Plus/protein A-agarose was obtained from Oncogene Science (Manhasset, NY), and horseradish peroxidase-conjugated anti-phosphotyrosine antibody, polyclonal antibodies against PARP (A-20) and lamin B, and monoclonal anti-H-Ras antibody were from Santa Cruz Biotechnology (Santa Cruz, CA). Polyclonal antibodies against ERK 1/2, Akt1 (no. 06-558), Akt2 (no. 06-606) and carboxyl-terminal IRS-1, recombinant histidine-tagged caspase-3, and N17Ras.pUSEamp+ vector were from Upstate Biotechnology (Lake Placid, NY). Phospho-specific anti-ERK 1/2 and phospho-Ser473 Akt antibodies were obtained from Promega Corp. (Madison, WI) and New England Biolabs, Inc. (Beverly, MA), respectively. Electrophoresis reagents, such as gels, Tris-glycine SDS running buffer, and poly(vinylidene difluoride) (PVDF) membrane were from Novex Corp. (San Diego, CA). Ham's F-12 medium, D-PBS, and Cell-stripper were from Cellgro (Freiburg, Germany), FBS was from Gemini (Calabasas, CA), and trypsin-EDTA was from NIH (Bethesda, MD).

Cell Culture. Cells used in this study were described previously (*12*, *17*) and include CHO-IR cells and CHO-IR cells expressing a deletion mutant of mSOS1 (CHO-IR/ΔSOS). CHO-IR/ΔSOS cells were from Dr. M. Sakaue (Kobe University, Kobe, Japan). Cells were grown in Ham's F-12 medium containing 100 units/mL penicillin, 100 μg/mL streptomycin, and 10% fetal bovine serum (FBS), and maintained in a humidified atmosphere of 5% CO_2 in air at 37 °C.

Treatments. CHO-IR and CHO-IR/ΔSOS cells were grown to confluence in 35-mm tissue culture dishes and then subjected to growth factor withdrawal in F-12 medium supplemented with 0.1% (w/v) bovine serum albumin for 3 h followed by the addition of 10 μM manumycin or vehicle (dimethyl sulfoxide) for 60 min prior to the addition of 10 nM insulin or 10% FBS. Eighteen hours later, floating cells were collected by centrifugation, harvested, and combined with the cells remaining attached to the plate.

Construction of pTracer.N17Ras.GFP. An expression vector that produces both the dominant negative N17 mutant of human H-Ras (N17Ras) and super-green fluorescent protein (GFP) was prepared by inserting full-length N17Ras cDNA fragment into pTracer.GFP plasmid as followed. The N17Ras cDNA fragment was excised from N17Ras.pUSEamp+ vector with *Kpn*I and *Eco*RV digestion, and the fragment (1.1 kb) was then inserted into pTracer.GFP vector, which was linearized with *Kpn*I/*Eco*RV, by ligation with T4 ligase (Pharmacia Biotech.). Competent DH5α bacterial cells were transformed with the ligated plasmid, selected with ampicillin and subjected to plasmid preparation. The presence of N17Ras cDNA was confirmed by *Kpn*I/*Eco*RV digestion. CHO cells were transiently transfected with pTracer expression vectors containing either GFP cDNA alone or together with N17Ras cDNA. Transfection was done with 1.0 μg of DNA by using the Lipofectamine-plus technique (Life Technologies, Gaithersburg, MD) according to the manufacturer's protocol. After incubation for 24 h in F-12 medium, the cells were incubated for an additional 18 h in serum-free medium supplemented or not with insulin or 10% FBS.

DNA Laddering. Internucleosomal DNA fragmentation analysis was performed essentially as described previously

(*17*). Briefly, pooled cellular DNA from adherent and detached cells was prepared using the Puregene Kit (Gentra Systems, Inc., Minneapolis, MN), and the purified DNA was then incubated with 20 μg/mL RNase A for 1 h at 37 °C. Equal amounts of DNA from each sample (0.5 μg) were 3′-OH-labeled with 5 units of Klenow fragment of DNA polymerase I (New England Biolabs) and 0.5 μCi [α-^{32}P]-dCTP (~3000 Ci/mmol, Amersham Corp., Arlington Heights, IL) and electrophoresed on 6% (w/v) polyacrylamide gel. DNA was visualized by autoradiography of the dried gel using Kodak BioMax film and intensifying screens.

Flow Cytometric Analysis. Protocol I. Upon induction of apoptosis, cytoplasmic phosphotidylserine translocates to the external surface of the cell membrane, allowing its in vitro detection through interaction with annexin V (*22*). Untreated cells or cells treated with manumycin, insulin, or FBS were harvested with Cell-stripper solution and combined with their medium to collect any detached cells. The cell suspension concentration was adjusted to ~1 × 10^6 cells/mL with D-PBS (Ca^{2+}/Mg^{2+} free); aliquots of cell suspension (5 × 10^5) were incubated at room temperature with media binding reagent and Annexin V-FITC as indicated by the manufacturer (Oncogene Research Products, Cambridge, MA). After 15 min in the dark, cells were centrifuged at 1000*g* for 5 min and the cell pellet resuspended in 500 μL of ice-cold binding buffer and 10 μL of 30 μg/mL PI supplied by the manufacturer. The samples were immediately analyzed by flow cytometry on a FACScan flow cytometer (Becton Dickinson, Cockeysville, MD) equipped with a 15 mW argon-ion laser. Ten thousand events were collected for each sample. An excitation wavelength of 488 nm was used while fluorescence emissions of 507 and 580 nm were collected to detect FITC and PI signals, respectively. The log of annexin V−FITC fluorescence was displayed on the *x*-axis and the log of PI fluorescence on the *y*-axis.

Protocol II. Cells were incubated with 60 μg/mL PI for 20 min and then detached from culture dishes using cell-stripper solution. The cells were collected by low speed centrifugation, washed twice in D-PBS followed by FACS analysis where 20 000 events were collected for each sample. An excitation wavelength of 488 nm and fluorescence emissions of 507 and 580 were used for the detection of GFP-expressing cells and PI-stained cells, respectively.

Protocol III. Cells were removed from the culture dish using a 0.05% (w/v) trypsin solution, washed twice in D-PBS and fixed in 70% (v/v) EtOH. The cells were incubated with 50 μg/mL PI in D-PBS and 20 μg/mL Rnase A for 30 min at room temperature, consistent with the staining technique originally described by Crissman and Steinkamp (*23*) to assess apoptosis. An excitation wavelength of 488 nm and fluorescence emission of 580 nm were used. The log of PI fluorescence was converted to linear fluoresence intensity.

Determination of Caspase-3 Activity. Cells were lysed in ice-cold 0.5 mL of buffer I [50 mM Tris.HCl, pH 7.4, 150 mM NaCl, 1% (w/v) NP-40, 0.25% (w/v) sodium deoxycholate, and 1 mM EGTA] for 15 min at 4 °C. After centrifugation at 10000*g* for 20 min at 4 °C, aliquots of supernatant were incubated with 25 μM Ac-DEVD-AMC for 3 h at 37 °C. Experiments were performed with a recombinant hexahistidine-tagged caspase-3 standard (0−2 ng/assay) to ensure that under these conditions the cleavage of the fluorogenic substrate was linear with respect to caspase-3 activity. The generation of fluorescent product was detected using excitation and emission wavelengths of 380 and 460 nm, respectively. Alternatively, a colorimetric assay was used where caspase-3 activity of the supernatants from cells lysed in modified buffer I (where EGTA was replaced with 1 mM EDTA) was measured by incubating cell lysates with reaction buffer [100 mM Hepes, pH 7.5, 20% (w/v) glycerol, 5 mM dithiothreitol, and 0.5 mM EDTA] containing 100 μM of the colorimetric substrate, Ac-DEVD-*p*NA. The release of *p*-nitroalinine was detected by monitoring absorbance at 405 nm for 30 min at 37 °C using a microtiter plate reader (Bio-Rad, Hercules, CA). In certain experiments, the cell lysate was first incubated with caspase-3 inhibitors (e.g., z-DEVD-fmk or DEVD-CHO).

Polyacrylamide Gel Electrophoresis and Western Blot Analysis. Unless otherwise indicated, cells were lysed directly in Laemmli sample buffer (*24*) containing 5% (v/v) 2-mercaptoethanol and 1 mM orthovanadate. After heating at 70 °C for 10 min, proteins were separated by SDS−PAGE on 4−12% polyacrylamide gradient gel along with prestained protein markers, and electrotransferred onto PVDF membrane. The membrane was incubated with blocking buffer [5% (w/v) nonfat dried milk in Tris-buffered saline (TBS)−0.1% (w/v) Tween-20 (TBS-T)] for 1 h at room temperature and then probed with a 1:48000 dilution of HRP-conjugated phosphotyrosine antibody in blocking buffer to detect changes in protein tyrosine phosphorylation. After a series of washes, positive signals were visualized with the enhanced chemiluminescence (ECL) reagents in combination with Hyperfilm-ECL (Amersham). Band intensities were quantitated by laser densitometry using the ImageQuant software (Molecular Dynamics, Sunnyvale, CA). The membranes were also reprobed with various primary antibodies (1:1000) followed by the appropriate HRP-conjugated secondary antibodies (1:3000).

In Vitro Binding of Active Ras to GST-RBD. GST-RBD was kindly provided by Dr. Johannes L. Bos (Utrecht University, Netherlands) and was used to determine the relative amount of active GTP-bound p21Ras, as previously described (*25*). The GST-RBD fusion protein contains the minimal Ras binding domain of Raf-1 (amino acids 51−131). The prokaryotic expression vector (pGEX-2T) containing sequences for a fusion protein of glutathione S-transferase (GST) and RBD was transformed into *E. coli* BL21 cells. These transformed cells were grown in LB medium and the induction of GST-RBD expression was carried out by addition of 0.2 mM isopropyl-β-thiogalactopropyranoside. After 4 h, cells were pelleted by centrifugation, suspended in PBS and then disrupted in B-PER reagent (Pierce, Rockford, IL). The cell lysate was centrifuged at 5000*g* for 5 min at 4 °C and Triton X-100 was added to the supernatant to reach a final concentration of 1% (w/v). After centrifugation at 12000*g* for 10 min at 4 °C, the supernatant was mixed with glycerol (10% final, w/v), aliquoted, and stored at −80 °C until use. Crude GST-RBD extract was incubated with glutathione-bound agarose 4B beads (Pharmacia, Uppsala, Sweden) for 30 min at 4 °C. The beads were recovered by centrifugation and washed twice with lysis buffer II [25 mM Hepes, pH 7.5, 150 mM NaCl, 1% (w/v) NP-40, 0.25% (w/v) sodium deoxycholate, 10% (w/v) glycerol, 25 mM NaF, 10 mM $MgCl_2$, 1 mM EDTA, 1 mM orthovanadate, 10 μg/mL leupeptin, and 10 μg/mL aprotinin].

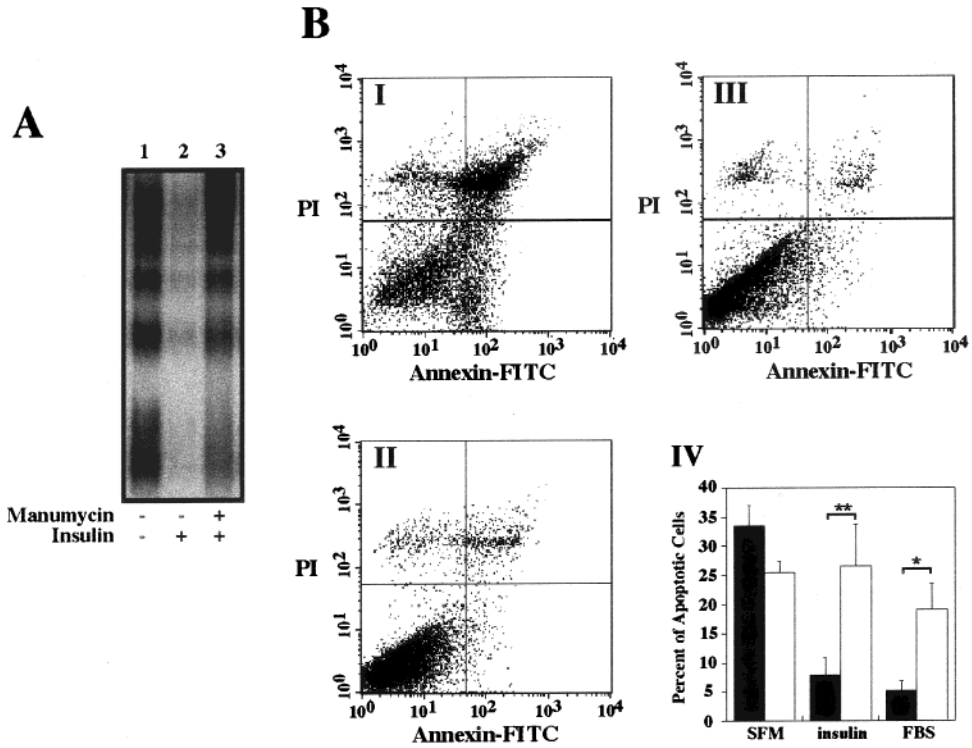

FIGURE 1: Pro-apoptotic role of manumycin in CHO-IR cells. (A) SFM-treated CHO-IR cells were incubated with 0.1% DMSO (control) or 10 μM manumycin for 1 h followed by a 16-h incubation in the absence or presence of 10 nM insulin. Genomic DNA was prepared and analyzed for internucleosomal DNA fragmentation as described in Materials and Methods. An autoradiogram of a representative DNA fragmentation analysis is shown. Similar results were obtained in at least five independent experiments. (B) Annexin V-FITC staining was performed on CHO-IR cells that were incubated for 18 h in SFM (panel I), 10 nM insulin (panel II) or 10% FBS (panel III) as described in Materials and Methods. Similar experiment were repeated with cells treated with manumycin alone or in combination with insulin or FBS. Panel IV, percent of apoptotic cells that were positively stained for PI and Annexin V-FITC is represented as the mean ± SE of three independent experiments. (*, **) $P < 0.05$ and 0.01. (■) Vehicle; (□) manumycin.

CHO-IR and CHO-IR/ΔSOS cells grown either on 35- or 60-mm dishes were lysed in 0.5 mL of lysis buffer II on ice, centrifuged at 10000*g* for 20 min, and the clarified lysates incubated with precoupled GST-RBD beads for 30 min at 4 °C. The beads were pelleted by centrifugation and washed three times in lysis buffer II before solubilization in Laemmli sample buffer. The samples were separated on a 16% SDS−PAGE gel under reducing conditions, and immunoblotted either with panRas, K-Ras, or H-Ras monoclonal antibodies (each at 2.5 μg/mL).

Statistical Analysis. Data are presented as the mean ± SEM. Comparison between groups were made by ANOVA coupled to Fisher's protected least significant differences *post-hoc* test.

RESULTS

CHO-IR cells were pretreated with manumycin, an analogue of farnesyl diphosphate, for 1 h followed by a 16-h incubation in the absence or presence of insulin or 10% FBS. The DNA laddering assay was then used to assess the presence of internucleosomal DNA fragmentation, one of the hallmark of apoptotic death (*26*). Manumycin blocked the ability of insulin (Figure 1A) and serum (data not shown) at reducing the formation of DNA fragments that were generated in response to serum withdrawal (SFM) (Figure 1A). To independently verify the pro-apoptotic role of manumycin, annexin V binding was then performed on live cells by flow cytometry. As control experiment, we noted that the proportion of apoptotic cells that were stained with annexin V-FITC and PI upon serum starvation was decreased from 33.4 ± 3.5 to 7.9 ± 3.1% and 5.3 ± 1.6% in the presence of 10 nM insulin and 10% FBS, respectively (mean ± SE, $n = 3$) (Figure 1B; upper right quadrant in panels I−III). Here pretreatment with 10 μM manumycin for 1 h rendered cells insensitive to the protection by insulin or FBS (Figure 1B; panel IV).

Initial Characterization of the Pro-Apoptotic Action of Manumycin in CHO-IR Cells. The caspase family of cysteine proteases plays a pivotal role in mediating apoptosis through the proteolysis of specific targets that include poly(ADP-ribose) polymerase (PARP) and the nuclear lamins (*27*). The function of caspase-3 (like) activity has been described to be involved in the execution of apoptosis in a tissue-, cell type-, or death stimulus-specific manner (*28*). Immunoblot analysis revealed that the combination of manumycin and insulin for 4 and 24 h markedly decreased the amount of lamin B and PARP proteins in whole cell lysates without altering the expression or integrity of ERK 1/ERK 2 (Figure 2A). CHO-IR cells were treated under various experimental conditions and activation of caspase-3 was then measured using the fluorogenic substrate, Ac-DEVD-AMC. Active caspase-3 cleaves Ac-DEVD-AMC, thus causing an increase in fluorescence intensity that can be quantitated. When SFM-treated cells were incubated in the presence of 10 nM insulin, the increase in fluorescence intensity was attenuated ~6-fold (Figure 2B). Pretreatment with manumycin blocked the reduction in caspase-3 activity by insulin. Similar results were obtained when using a colorimetric assay for determining

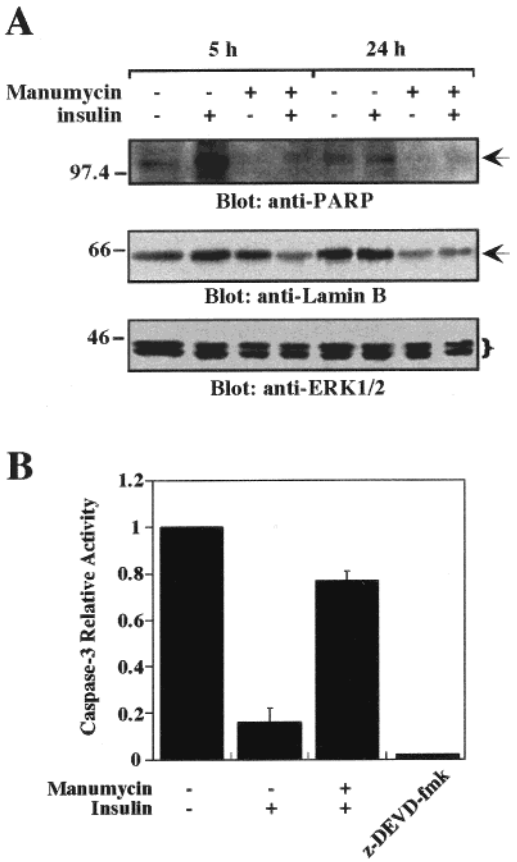

FIGURE 2: Western blot analysis and caspase-3 activity in manumycin-treated cells. (A) SFM-treated CHO-IR cells were incubated with vehicle or 10 μM manumycin for 1 h followed by the addition of 10 nM insulin for 5 or 24 h. Whole cell lysates were prepared and loaded on a gradient SDS−polyacrylamide gel. Following electrophoresis under reducing conditions, the gel was transferred to PVDF membrane and immunoblotted with antibodies against PARP, lamin B, and ERK 1/ERK2. Molecular mass markers are shown on the left in kilodaltons. (B) Control and manumycin-treated cells were incubated with 10 nM insulin where indicated or with 20 μM z-DEVD-fmk. Eighteen hours later, cells were harvested and caspase-3 activity was measured by using the fluorescent substrate Ac-DEVD-AMC. Results are expressed as mean ± SD of four independent observations.

caspase-3 activity (data not shown). Addition of the cell-permeant z-DEVD-fmk (20 μM) (*29*) markedly inhibited caspase-3 activity (Figure 2B), demonstrating the specific nature of this assay.

Role of p21Ras in Insulin-Mediated Increase in Cell Survival. We investigated, next, whether manumycin's ability to antagonize insulin survival function was the result of p21Ras inhibition. Increased farnesyltransferase activity results in a larger pool of farnesylated p21Ras to the plasma membrane and allows for enhanced GTP loading carried out through the exchange of GDP to GTP by Ras-specific exchange factors (*30*). To confirm the selective effect of manumycin on p21Ras processing and localization, CHO-IR cells were fractionated into a particulate fraction (100000*g* pellet) enriched in cellular membranes and a cytosolic fraction, and their content in H- and K-Ras isoforms was analyzed by Western blot. Control experiments with total lysates and membrane fractions showed a very low abundance of endogenous H-Ras whereas K-Ras was readily detectable (data not shown). We found that the association of K-Ras proteins with the particulate fraction was not

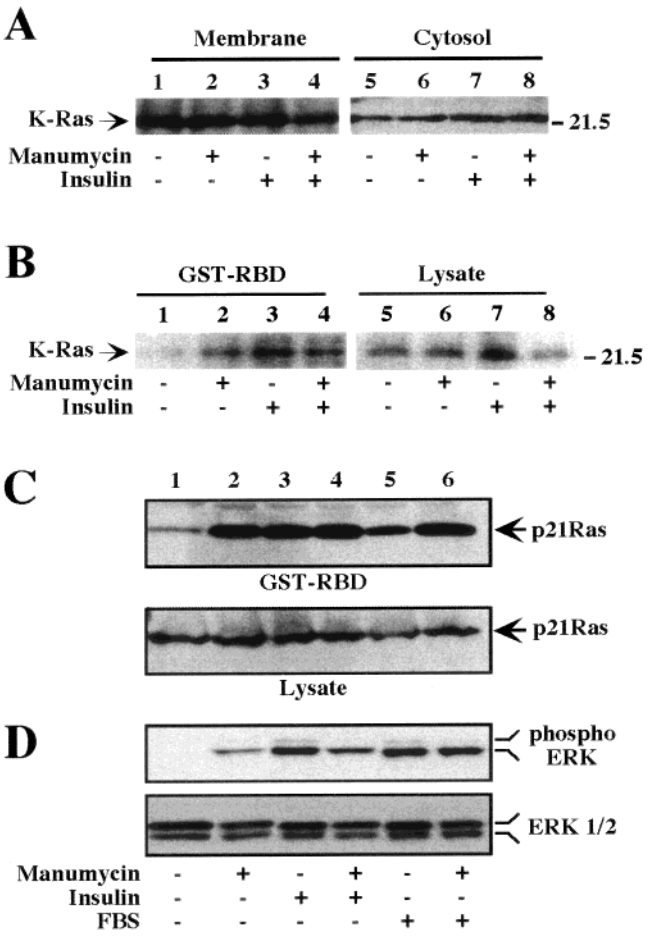

FIGURE 3: Effect of manumycin on membrane association and activation of p21Ras, and ERK dual phosphorylation. (A) SFM-treated CHO-IR cells were preincubated with 0.1% DMSO or 10 μM manumycin for 1 h followed by the addition of vehicle or 10 nM insulin for 18 h. Cell lysates were fractionated into a membrane-enriched particulate fraction and a cytosolic fraction (supernatant 100000*g*), and immunoblotted with anti-K-Ras antibody. (B) Following an 18-h preincubation period in the absence or the presence of 10 μM manumycin, CHO-IR cells were maintained in SFM for 4 h without or with manumycin, followed by the addition of vehicle or 10 nM insulin for 5 min. Cell lysates were prepared and incubated in the presence of GST-RBD fusion protein, as described in Materials and Methods. The samples were electrophoresed and then immunoblotted with a K-Ras antibody. (Left panel) A representative immunoblot is shown; (right panel) whole cell lysate from each treatment group was immunoblotted with the same antibody. (C) Lysates from manumycin-treated cells stimulated or not with insulin or 10% FBS for 5 min were incubated with GST-RBD fusion protein, and the immobilized proteins were immunoblotted with a pan-Ras antibody. (D) Whole cell lysates were prepared and immunoblotted with antibodies against dually phosphorylated ERK 1/2 (upper panel). (Lower panel) The same membrane was then reprobed with anti-ERK 1/2 antibodies. Similar results were obtained in three independent experiments.

affected by manumycin, insulin, or the combination manumycin plus insulin (Figure 3A).

To assess whether manumycin can inhibit insulin-stimulated K-Ras function, extracts from treated cells were incubated with the Ras-binding domain (RBD) of Raf-1 to precipitate GTP-bound p21Ras (e.g., activated state) (*25*) followed by detection of K-Ras proteins by Western blot analysis. In the absence of insulin, continuous manumycin (10 μM) treatment for 18 h caused an increase in the amount of K-Ras proteins precipitated with GST-RBD (Figure 3B, lanes 2 vs 1). Acute stimulation with insulin for 5 min raised

the level of active RBD-interacting K-Ras proteins several-fold above basal levels (Figure 3B, lanes 3 vs 1). This increase was only marginally reduced in the presence of manumycin. Comparable amount of K-Ras proteins was present in total cell lysates (Figure 3B, right panel), indicating no significant effect of manumycin on Ras expression. In a second set of experiments, membranes were probed with a panRas antibody that recognizes various Ras isoforms. As shown in Figure 3C, the ability of insulin or 10% FBS to acutely stimulate Ras interaction with GST-RBD was maintained in the presence of manumycin. Recall that K-Ras proteins are far more abundant than H-Ras in CHO-IR cells (see above), suggesting that the signals generated with panRas antibody may be derived from K-Ras. As shown in Figure 3D (upper panel), manumycin increased basal ERK activity as determined by the use of phospho-specific ERK 1/ERK 2 antibodies. The insulin-mediated activation of ERK was attenuated somewhat in manumycin-treated cells. In contrast, manumycin had no apparent effect on ERK activation by 10% FBS. Taken together, these findings provide evidence that induction of apoptosis by manumycin was not the result of K-Ras inhibition and/or alteration in the Ras/Raf-1/ERK signaling pathway.

Antiapoptotic Function of Insulin in CHO-IR/ΔSOS Cells. The importance of p21Ras activation in the survival function of insulin was examined further by using CHO-IR cells transfected with ΔSOS, a transdominant negative mutant of the Ras-specific exchange factor, SOS1. We first assessed the impact of ΔSOS on the content of Ras proteins immobilized by GST-RBD in response to insulin. Short-term exposure to 10 nM insulin resulted in a large increase in the amount of GTP-bound Ras precipitable with GST-RBD in CHO-IR cells but not in CHO-IR/ΔSOS cells (Figure 4A). This result was independently confirmed by showing that expression of ΔSOS in CHO-IR cells inhibited insulin-mediated increase in Raf-1 activity in vitro (data not shown). To test whether insulin responses that are dependent on Ras would be abrogated in CHO-IR/ΔSOS cells, whole cell extracts were analyzed by SDS−polyacrylamide gel electrophoresis and immunoblotting. Insulin treatment raised the level of tyrosine phosphorylation of pp185 (e.g., IRS-1) but failed to promote ERK activation, as assessed by reprobing the membrane with phosphospecific anti-ERK 1/ERK2 antibody (Figure 4B), while causing marked elevation in the PI 3-kinase/Akt pathway (data not shown). In contrast, a 5-min incubation with 10% FBS had no effect toward IRS-1 phosphorylation but caused substantial increase in ERK dual phosphorylation both in CHO-IR and CHO-IR/ΔSOS cells (Figure 4B, lanes 3 vs 6). These observations support the notion that insulin-mediated activation of the Ras/Raf-1/ERK signaling cascade is selectively abolished in CHO-IR/ΔSOS cells. The results from flow cytometry analysis indicated that, despite abrogation of the Ras/ERK pathway, insulin (10 nM) exerted potent antiapoptotic protection in SFM-treated CHO-IR/ΔSOS cells, as evidenced by the marked reduction in signal in subG1 phase, a region corresponding to apoptotic cells (<2N DNA content) (Figure 4C, I—I). Addition of manumycin rendered these cells insensitive to the survival function of insulin or serum (data not shown).

Taken together, our results demonstrate that the pro-apoptotic role of manumycin cannot be ascribed to alteration in K-Ras-mediated signaling. Since the various Ras isoforms interact with distinct signaling pathways within the cell, we next assessed the impact that expression of human (dominant negative) H-Ras^{N17} will have on the survival function of insulin. Transient expression of a plasmid encoding either the GFP protein alone or GFP and H-Ras^{N17} proteins was carried out in CHO-IR and CHO-IR/ΔSOS cells. H-Ras^{N17}-expressing cells and control cells (GFP alone) were maintained in SFM or stimulated with insulin (10 nM) or 10% FBS for 18 h. Propidium iodide-stained cells were then analyzed for the expression of GFP protein (detected by green fluorescence) by flow cytometry. The addition of

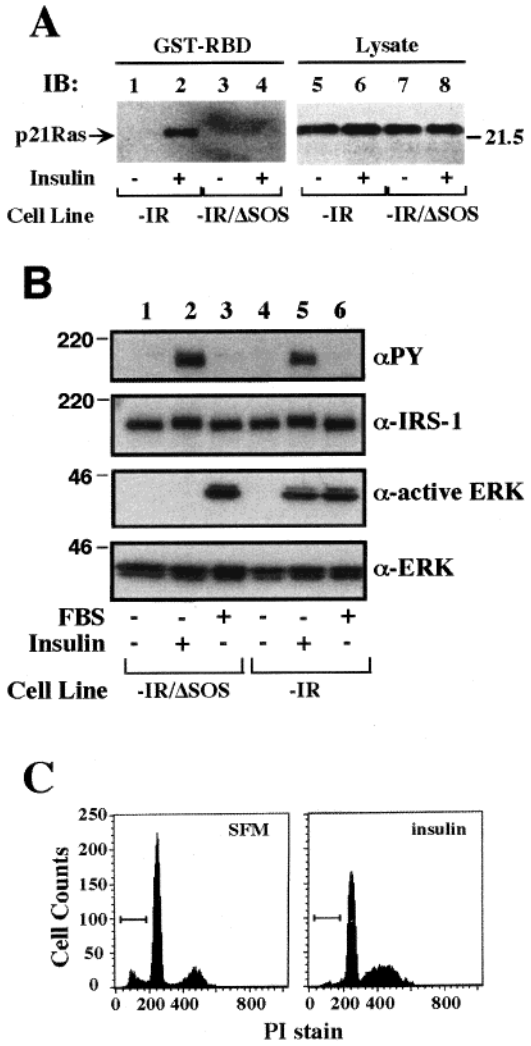

FIGURE 4: Impaired activation of the Ras/Raf-1/ERK cascade by insulin in CHO-IR/ΔSOS cells. (A) Serum-starved CHO-IR and CHO-IR/ΔSOS cells were incubated with vehicle or 10 nM insulin for 5 min, and then lysed. After incubating each cell lysate with GST-RBD fusion protein, the immobilized proteins were immunoblotted with pan-ras antibody as described in the legend of Figure 3. (B) SFM-treated cells were incubated with vehicle, 10 nM insulin or 10% FBS for 5 min at 37 °C. Whole cell lysates were prepared and immunoblotted with antibodies specific for phosphotyrosine (PY), IRS-1, or the dually phosphorylated ERK. The same blot was also probed with anti-ERK 1/2 antibody to confirm that equal amounts of protein were loaded in each lane. (C) Analysis of apoptotic death using flow cytometry. Following a 18-h treatment with SFM or 10 nM insulin, adherent and detached CHO-IR/ΔSOS cells were pooled, stained with PI and analyzed for DNA content. A constant number of events (10 000) were analyzed per sample. Apoptotic cells with DNA content of <2*N* are marked by "I—I". At least four separate experiments were carried out with comparable results.

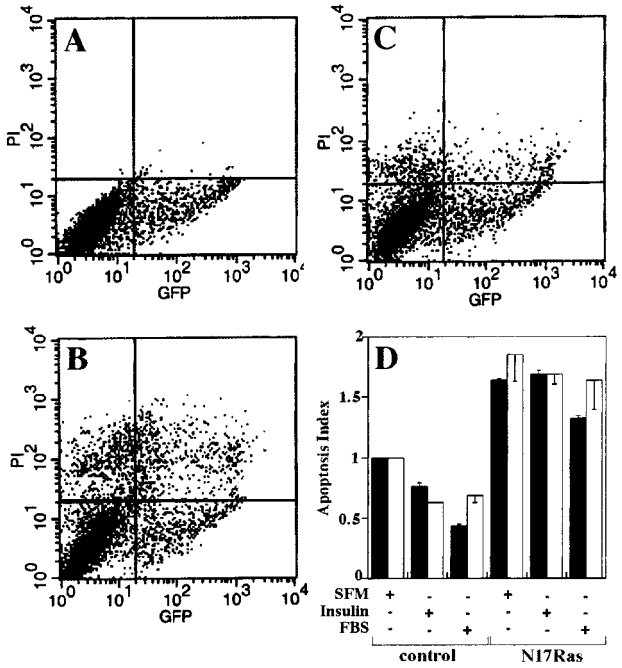

FIGURE 5: H-Ras-dependent antiapoptotic protection. CHO-IR cells were transiently transfected with an expression vector encoding either the GFP protein alone or GFP and Ras^{N17} proteins. After 24 h, the cells were serum-starved and then incubated in the absence (SFM) or the presence of insulin or 10% FBS for 18 h. The cells were subsequently processed for flow cytometry analysis as described in the Experimental Procedures. The quadrant markers for the bivariate dot plots were set based on the serum-treated GFP control without PI staining (panel A). (B) SFM-treated GFP control; (C) serum-treated GFP control; (D) the data represent the mean ± range of two independent experiments, where the relative level of apoptosis in SFM-treated GFP controls was arbitrarily set at 1.0. (□) CHO-IR cells; (■) CHO-IR/ΔSOS cells.

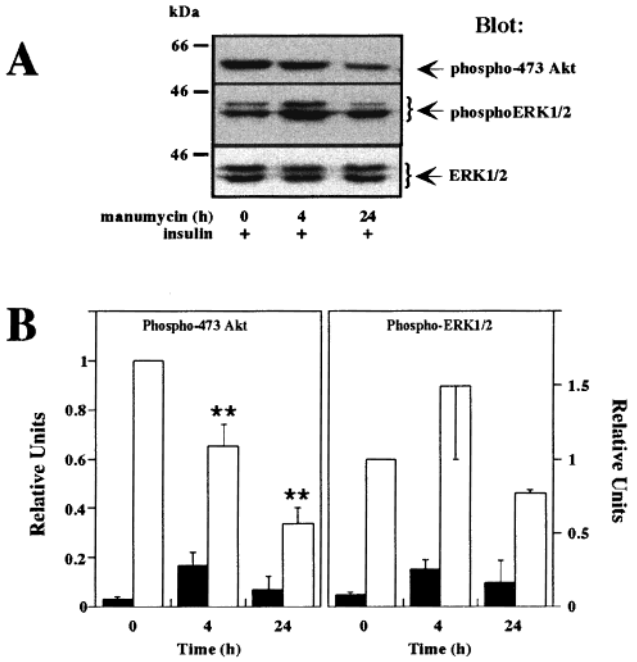

FIGURE 6: Manumycin inhibits insulin-mediated increase in Akt phosphorylation at Ser473. Serum-starved CHO-IR cells were incubated with vehicle or 10 μM manumycin for 4 and 24 h followed by the addtion of 10 nM insulin where indicated. Ten minutes later, cells were lysed and the content in phosphorylated Akt and ERK was analyzed by immunoblotting using phospho-specific antibodies. (A) Blot from a representative experiment is shown. (B) The data represent the mean ± SE of four to five independent observations, where the relative level of phospho-473 Akt (left panel) and dually phosphorylated ERK 1/2 (right panel) was arbitrarily set at 1.0. (**) $P < 0.01$ when compared to insulin alone. (■) No insulin; (□) insulin-treated cells.

10% serum reduced SFM-mediated apoptosis in control cells expressing GFP alone (Figure 5B vs C, upper right quadrants). In cells transfected with GFP and $H\text{-}Ras^{N17}$ proteins, there was a ~1.6-fold increase in the extent of apoptotic death in response to SFM and a complete abolition of cell survival by insulin or serum (Figure 5D). The cellular expression of human $H\text{-}Ras^{N17}$ was confirmed by immunoblot analysis (data not shown).

Manumycin Inhibits Insulin-Induced Akt Activation. The activation of PKB/Akt by phosphorylation plays a major role in cell survival by inhibiting apoptosis mediated by a number of stimuli, including SFM (*31*). Because of the exquisite sensitivity of H-Ras to farnesylation inhibitors (*18*, *19*) and its ability to potently stimulate the PI 3-kinase/Akt pathway (*21*), we tested for changes in phospho-Akt levels between manumycin-treated cells and control cells in the absence or presence of insulin. Serum-starved CHO-IR cells were treated with 10 μM manumycin for 4 and 24 h prior to insulin stimulation for 10 min. Aliquots of cell lysate were electrophoresed and then immunoblotted with an anti-phosphospecific Akt antibody that recognize Akt that had been phosphorylated at Ser473 (Figure 6A). Cell treatment with manumycin resulted in a significant reduction in insulin-mediated Akt phosphorylation (35 ± 4 and 66 ± 10% inhibition after 4 and 24 h treatment, respectively; $P < 0.01$, $n = 4-5$) (Figure 6B, left panel) despite similar levels of ERK dual phosphorylation (Figure 6B, right panel). This implies that activation of H-Ras/PI 3-kinase/Akt pathway may be impaired in manumycin-treated cells. Similar findings were obtained with another specific farnesyltransferase inhibitor, FTI-277. The addition of FTI-277 (1 μM) to SFM-treated CHO-IR cells for 4 h led to a 44 ± 7% inhibition of insulin-mediated Akt phosphorylation ($n = 2$) without altering ERK dual phosphorylation following treatment with insulin (data not shown). Immunoprecipitation-based kinase assay with crosstide as substrate confirmed that insulin-mediated increase in Akt activity was reduced by ~50% after 4 h treatment with manumycin (data not shown). These results indicate that a short-lived farnesylated protein(s) may be involved in the activation of Akt.

DISCUSSION

In this report, it was observed that manumycin influences apoptosis in a way that sharply differs from that mediated by growth factor deprivation. Insulin, 10% FBS, or antioxidants (our unpublished data) can markedly reduce apoptosis mediated by serum starvation in CHO-IR cells. In contrast, cells that were pretreated with manumycin could not be rescued from apoptotic death in response to insulin and other survival factors. This FTI caused also 3T3-L1 fibroblasts to undergo apoptosis despite cell treatment with 10% serum (our unpublished data). Our results differ from those of Suzuki et al. (*32*) who showed that FTIs preferentially induce apoptosis in Ras-transformed normal rat kidney (KNRK) cells but not in untransformed cells and that the presence of 10% serum counteracts FTI-induced apoptosis. It is important to note that the KNRK cells were incubated with 80−100

μM FTIs for 36 h prior to analysis (*32*), conditions that are far more stringent than the ones used in the work herein. Moreover, the concentrations of manumycin used in our studies (5−20 μM) have been reported to selectively inhibit farnesyltransferase (IC_{50} = 5−10 μM) but not geranylgeranyltransferases (IC_{50} = 180 μM) (*33*). In support of our earlier observation, we incubated CHO-IR cells with two other FTIs (FTI-277 and α-hydroxyfarnesylphosphonic acid) at concentrations ranging from 1 to 10 μM in the presence of 10 nM insulin for 16 h and found an induction of apoptosis although to a lesser degree than that observed with manumycin.[2]

By competing with normal Ras for binding to specific guanine-nucleotide-exchange factors, the dominant negative mutant of H-Ras (Ras^{N17}) prevents the activation of endogenous Ras and its interaction with downstream target proteins. We found that transient expression of Ras^{N17} exerted significant loss in the ability of insulin and serum to confer antiapoptotic protection, indicating that Ras and/or its downstream target proteins may play an important survival function. Although several Ras isoforms are expressed ubiquitously and can activate the same effector pathways, quantitative differences exist in their ability to stimulate Raf-1/ERK cascade and the PI 3-kinase/Akt pathway. The recruitment of Raf-1 to the plasma membrane and its subsequent activation are influenced to a greater extent by K-Ras proteins, whereas H-Ras is a more potent activator of PI 3-kinase (*21*). Furthermore, Ras isoforms vary in their sensitivity to FTIs as suggested by the observation that K-Ras proteins, but not H-Ras, remain attached to the plasma membrane following cell treatment with FTI (*18*, *19*). In the present study, evidence was provided to suggest that the K-Ras/Raf-1/ERK cascade is not the target of manumycin's pro-apoptotic action in CHO-IR cells. We have shown that endogenous K-Ras protein remains associated with the membrane fraction and that its activation in term of GST-RBD binding and ERK dual phosphorylation is not blocked by manumycin. Our results demonstrate also that there is an increase in the level of K-Ras•GTP complex and ERK activation between control cells and cells treated with manumycin alone. This implies that blocking protein farnesylation can relieve a basal inhibitory "tone" on K-Ras-mediated events, presumably at a step uptream of K-Ras. These results indicate that manumycin may target farnesylated protein(s) whose function includes the regulation of IR antiapoptotic pathway. As indicated earlier, it has been shown that FTIs selectively inhibit H-Ras prenylation thereby blocking H-Ras signaling and transformation (*34*). It is possible that manumycin induces apoptosis by targeting H-Ras; however, because of the long half-life of membrane-associated farnesylated Ras (∼24 h, ref *16*), farnesylated protein(s) other than H-Ras may be responsible for antiapoptotic control. Rho B has a short half-life (∼2 h) and is part of the immediate-early inducible response to growth factors and protein tyrosine kinases (*35*, *36*). The ability of FTIs to inhibit cell growth and Ras-dependent cell transformation is mediated by targeting the farnesylated RhoB protein (*36*, *37*). Thus, investigations of the involvement of RhoB and other small GTPases that are known to be essential in Ras transformation (e.g., RhoA, Rac1) (*38*) are required for a better understanding of the mechanism of manumycin-induced apoptosis in untransformed CHO-IR cells.

CHO-IR/ΔSOS cells were used to further support the notion that the Ras/Raf-1/MEK/ERK cascade plays no significant role in the antiapoptotic function of insulin. A feature of these cells include the ability of lysophosphatidic acid to potently stimulate ERK activity while being ineffective at reversing SFM-mediated apoptosis (our unpublished data). In this cell model, insulin confers antiapoptotic protection despite its inability to increase Raf-1 activity and ERK activation, indicating that stimulation of the Raf-1/MEK/ERK signaling pathway does not participate in the survival function of insulin. Other features of CHO-IR/ΔSOS cells include their sensitivity to manumycin pro-apoptotic action and their expression of a mutated SOS1 protein that lacks the guanine nucleotide exchange domain of Ras. Despite being unable to activate p21Ras, SOS1 mutant still can bind Grb2 (*12*) and thus may allow the association of the Grb2•ΔSOS heteroduplex with other signaling molecules that are implicated in control of cell death, which include Crk (*39*, *40*), and focal adhesion kinase (*41*−*44*), a widely expressed cytosolic tyrosine kinase. A model has been recently proposed whereby dephosphorylation of the focal adhesion kinase precedes caspase-mediated proteolysis of focal adhesion components and cell commitment to the initiation and execution of apoptosis (*42*). It would be of interest to determine whether a mechanism for manumycin-induced apoptosis involves inhibition of adhesion pathways.

The activation of Akt by phosphorylation plays a major role in cell survival by inhibiting apoptosis mediated by a number of stimuli, including SFM (*31*). Engagement of p21Ras by growth factors activates PI 3-kinase, which in turn promotes Akt phosphorylation by PDK1 and PDK2 (*45*). Akt is maximally activated at the plasma membrane by the phosphorylation of residues Thr308 and Ser473 (*45*). Of interest, growth factor-induced activation of AKT2, a member of the Akt family, can be blocked by cellular expression of a dominant-negative form of H-Ras (*46*, *47*). Thus, one can speculate that transient expression of $H\text{-}Ras^{N17}$ rendered CHO-IR and CHO-IR/ΔSOS cells insensitive to the pro-survival actions of insulin or serum through alteration of ligand-mediated Akt activation. However, the demonstration that manumycin and FTI-277 inhibit insulin-mediated Akt activation in CHO-IR cells within few hours is indicative of a kinetic that is too rapid to be explained by inhibition of Ras farnesylation. Because neither farnesylated RhoB nor two other small GTPases (e.g., Rac1 and RhoA) appear to be involved in Akt activation (*46*), our results indicate the need to identify and further investigate the role of short-lived farnesylated protein(s) that participate in insulin-mediated activation of Akt and its downstream antiapoptotic function.

In summary, we have shown that pharmacological inhibition of protein farnesylation with manumycin and other FTIs blocked insulin-mediated Akt phosphorylation and activation while maintaining intact the K-Ras/Raf-1/MEK/ERK cascade. The inhibition of insulin-stimulated Akt activity was rapid and preceded suppression of cell survival in untransformed CHO-IR cells.

[2] D. Park and M. Bernier, unpublished observations.

ACKNOWLEDGMENT

We thank Francis J. Chrest for FACS analysis, and Drs. Motoyoshi Sakaue and Johannes L. Bos for providing reagents. We also thank Dr. Ronald Wange for his assistance in implementing the Ras binding assay.

REFERENCES

1. Signore, A., Annovazzi, A., Gradini, R., Liddi, R., and Ruberti, G. (1998) *Diabetes Metab. Rev. 14*, 197−206.
2. Srinivasan, S., Stevens, M. J., Sheng, H., Hall, K. E., and Wiley, J. W. (1998) *J. Clin. Invest. 102*, 1454−1462.
3. Diaz, B., Pimentel, B., De Pablo, F., and De La Rosa, E. J. (1999) *Eur. J. Neurosci. 11*, 1624−1632.
4. Bertrand, F., Atfi, A., Cadoret, A., L'Allemain, G., Robin, H., Lascols, O., Capeau, J., and Cherqui, G. (1998) *J. Biol. Chem. 273*, 2931−2938.
5. Yenush, L., Zanella, C., Uchida, T., Bernal, D., and White, M. F. (1998) *Mol. Cell. Biol. 18*, 6784−6794.
6. Kummer, J. L., Rao, P. K., and Heidenreich, K. A. (1997) *J. Biol. Chem. 272*, 20490−20494.
7. Rampalli, A. M., and Zelenka, P. S. (1995) *Cell Growth Differ. 6*, 945−953.
8. Jarpe, M. B., Widmann, C., Knall, C., Schlesinger, T. K., Gibson, S., Yujiri, T., Fanger, G. R., Gelfand, E. W., and Johnson, G. L. (1998) *Oncogene 17*, 1475−1482.
9. Backer, J. M., Myers, M. G. Jr., Shoelson, S. E., Chin, D. J., Sun, X. J., Miralpeix, M., Hu, P., Margolis, B., Skolnik, E. Y., and Schlessinger, J., et al. (1992) *EMBO J. 11*, 3469−3479.
10. Ouwens, D. M., van der Zon, G. C., Pronk, G. J., Bos, J. L., Moller, W., Cheatham, B., Kahn, C. R., and Maassen, J. A. (1994) *J. Biol. Chem. 269*, 33116−33122.
11. Sasaoka, T., Draznin, B., Leitner, J. W., Langlois, W. J., and Olefsky, J. M. (1994) *J. Biol. Chem. 269*, 10734−10738.
12. Sakaue, M., Bowtell, D., and Kasuga, M. (1995) *Mol. Cell. Biol. 15*, 379−388.
13. Seger, R., and Krebs, E. G. (1995) *FASEB J. 9*, 726−735.
14. Rodriguez-Viciana, P., Warne, P. H., Dhand, R., Vanhaesebroeck, B., Gout, I., Fry, M. J., Waterfield, M. D., and Downward, J. (1994) *Nature 370*, 527−532.
15. Goalstone, M. L., and Draznin, B. (1996) *J. Biol. Chem. 271*, 27585−27589.
16. Goalstone, M., Leitner, J. W., and Draznin, B. (1997) *Biochem. Biophys. Res. Commun. 239*, 42−45.
17. Lee-Kwon, W., Park, D., Baskar, P. V., Kole, S., and Bernier, M. (1998) *Biochemistry 37*, 15747−15757.
18. Whyte, D. B., Kirschmeier, P., Hockenberry, T. N., Nunez-Oliva, I., James, L., Catino, J. J., Bishop, W. R., and Pai, J. K. (1997) *J. Biol. Chem. 272*, 14459−14464.
19. Rowell, C. A., Kowalczyk, J. J., Lewis, M. D., and Garcia, A. M. (1997) *J. Biol. Chem. 272*, 14093−14097.
20. Cox, A. D., and Der, C. J. (1997) *Biochim. Biophys. Acta 1333*, F51−F71.
21. Yan, J., Roy, S., Apolloni, A., Lane, A., and Hancock, J. F. (1998) *J. Biol. Chem. 273*, 24052−24056.
22. Boersma, A. W., Nooter, K., Oostrum, R. G., and Stoter, G. (1996) *Cytometry 24*, 123−130.
23. Crissman, H. A., and Steinkamp, J. A. (1973) *J. Cell Biol. 59*, 766−771.
24. Laemmli, U. K. (1970) *Nature 227*, 680−685.
25. de Rooij, J., and Bos, J. L. (1997) *Oncogene 14*, 623−625.
26. Wyllie, A. H. (1993) *Br. J. Cancer. 67*, 205−208.
27. Stennicke, H. R., and Salvesen, G. S. (1998) *Biochim. Biophys. Acta 1387*, 17−31.
28. Porter, A. G., and Janicke, R. U. (1999) *Cell Death Differ 6*, 99−104.
29. Pastorino, J. G., Chen, S. T., Tafani, M., Snyder, J. W., and Farber, J. L. (1998) *J. Biol. Chem. 273*, 7770−7775.
30. Zhang, F. L., and Casey, P. J. (1996) *Annu. Rev. Biochem. 65*, 241−269.
31. Downward, J. (1998) *Curr. Opin. Cell Biol. 10*, 262−267.
32. Suzuki, N., Urano, J., and Tamanoi, F. (1998) *Proc. Natl. Acad. Sci. U.S.A. 95*, 15356−15361.
33. Hara, M., Akasaka, K., Akinaga, S., Okabe, M., Nakano, H., Gomez, R., Wood, D., Uh, M., and Tamanoi, F. (1993) *Proc. Natl. Acad. Sci. U.S.A. 90*, 2281−2285.
34. Manne, V., Yan, N., Carboni, J. M., Tuomari, A. V., Ricca, C. S., Brown, J. G., Andahazy, M. L., Schmidt, R. J., Patel, D., and Zahler, R., et al. (1995) *Oncogene 10*, 1763−1779.
35. Jahner, D., and Hunter, T. (1991) *Mol. Cell Biol. 11*, 3682−3690.
36. Du, W., Lebowitz, P. F., and Prendergast, G. C. (1999) *Mol. Cell Biol. 19*, 1831−1840.
37. Lebowitz, P. F., Davide, J. P., and Prendergast, G. C. (1995) *Mol. Cell Biol. 15*, 6613−6622.
38. Khosravi-Far, R., Solski, P. A., Clark, G. J., Kinch, M. S., and Der, C. J. (1995) *Mol. Cell Biol. 15*, 6443−6453.
39. Evans, E. K., Lu, W., Strum, S. L., Mayer, B. J., and Kornbluth, S. (1997) *EMBO J. 16*, 230−241.
40. Pàrrizas, M., Blakesley, V. A., Beitner-Johnson, D., and Le Roith, D. (1997) *Biochem. Biophys. Res. Commun. 234*, 616−620.
41. Frisch, S. M., Vuori, K., Ruoslahti, E., and Chan-Hui, P. Y. (1996) *J. Cell Biol. 134*, 793−799.
42. Sonoda, Y., Kasahara, T., Yokota-Aizu, E., Ueno, M., and Watanabe, S. (1997) *Biochem. Biophys. Res. Commun. 241*, 769−774.
43. van de Water, B., Nagelkerke, J. F., and Stevens, J. L. (1999) *J. Biol. Chem. 274*, 13328−13337.
44. Guan, J. L. (1997) *Int. J. Biochem. Cell Biol. 29*, 1085−1096.
45. Balendran, A., Casamayor, A., Deak, M., Paterson, A., Gaffney, P., Currie, R., Downes, C. P., and Alessi, D. R. (1999) *Curr. Biol. 9*, 393−404.
46. Jiang, K., Coppola, D., Crespo, N. C., Nicosia, S. V., Hamilton, A. D., Sebti, S. M., and Cheng, J. Q. (2000) *Mol. Cell Biol. 20*, 139−148.
47. Liu, A. X., Testa, J. R., Hamilton, T. C., Jove, R., Nicosia, S. V., and Cheng, J. Q. (1998) *Cancer Res. 58*, 2973−2977.

BI000995Y